

Design and Setup of a New HPGe Detector Based Body Counter Capable of Detecting Also Low Energy Photon Emitters

O. Marzocchi¹, B. Breustedt¹, D. Mostacci², M. Urban³

¹ Institut für Nukleare Entsorgung, Karlsruher Institute of Technology (Hermann-von-Helmholtz-Platz 1, 76344 Eggenstein-Leopoldshafen, Germany)

² DIENCA Department, University of Bologna (Viale Risorgimento 2, 40136 Bologna, Italy)

³ Wiederaufarbeitungsanlage Karlsruhe Rückbau- und Entsorgungs-GmbH (Postfach 1263, 76339 Eggenstein-Leopoldshafen, Germany)

Keywords

Monte Carlo modeling, Partial-/Whole-body counter development, numerical phantoms, HPGe detectors

Abstract

Germanium detectors allow for an accurate detection of complex contamination cases involving multiple nuclides, but they are available in smaller sizes than scintillators and therefore require careful optimisation of the counting configuration. This work describes the complete redesign of the partial-body and whole-body counter installed at IVM (KIT, Karlsruhe) and the first results of its application. To speed up the design process, each detector was modelled using MCNPX and the validated models used for all the subsequent steps.

The definition of the partial-body counting configurations was performed exclusively with the help of simulations of voxel models of the human body: the photon fluxes around it were tracked and the detectors placed in the optimal positions. The configurations obtained were used as guideline to define the supporting mechanics.

The development of a whole-body counting (WBC) configuration was also performed using MC simulations and the photon flux, but in this case different results for different organs, phantoms and energies were aggregated to calculate average values and standard deviation. These two new quantities were used to optimise the setup.

Once the system and the mechanics were ready, different tests were performed. First, a reference phantom was used to quantify the improvement in the detection limit compared to the previous system. Later, two subjects potentially contaminated with ²¹⁰Pb were measured on the skull. This test aimed to check the lowest-energies capabilities of the system (46 keV). A last test involved the measurement of subjects returning from Japan after the Fukushima accident, with mixed results.

1 Introduction

Radiological risks come from different sources, both from work and natural environments. Some examples are industries using radioactive sources to study defects in the metals, medical applications of radioisotopes, and the process of decommissioning of nuclear reactors, during which radioactive powders may be generated. These particles are at risk of incorporation through inhalation, but in other cases the incorporation path could be ingestion or via wounds. Radiological risks are also originated in the natural environment: the radon gas is often the most significant source of radiological exposure to the population, due to inhalation and incorporation of itself or of some of its decay products. In some cases measuring the amount of one of them, namely ^{210}Pb , can help assess previous radon exposure. The new counter was designed to be able to measure the ^{210}Pb -content of the body via the 46.5 keV gamma emission.

The current system installed at the in vivo monitoring laboratory (IVM) of the Karlsruhe Institute of Technology (KIT) is used for the monitoring of workers at KIT campus and for external customers. IVM is an approved lab for individual monitoring according to German regulation, it maintains a quality management system and is accredited to ISO/IEC 17025:2005. The laboratory is also involved in scientific studies and the education and training of students and radiation protection workers.

The performances of the pre-existing system are acceptable thanks to the mass of the crystal (20 cm diameter, 10 cm depth) that ensured high counting efficiency, but the poor ability to detect complex contamination cases was a limiting factor (e.g. ^{40}K and ^{60}Co peaks overlap). The also available (PBC) body counting system, based on similarly sized phoswich detectors optimized for low-energy applications, suffered the same problem: for example, the evaluation of cases with both ^{239}Pu and ^{241}Am was difficult.

To overcome these limitations, an upgrade with a set of four 80% efficiency HPGe detectors was planned. The main advantage is the improved resolution, from 10-30 keV of the phoswiches to 0.9-2.5 keV of the HPGe (10 times or better improvement), but the choice of a digital electronics module, instead of analog alternatives, also eases the calibration, thanks to higher temperature stability. HPGe detectors usually require nitrogen cooling, a significant disadvantage, but the model chosen uses an electrical compressor to cool the crystal, resulting in continuity of operation with only the aid of a UPS system. The low-energy performances, usually poor in p+ coaxial crystals, are also avoided by the use of a "XtRa" configuration, where the front dead layer is mechanically removed and the energy range is extended down to 5 keV (a carbon epoxy window is used instead of beryllium, see [2]).

2 Characterization of the detectors

The optimization of the counting configurations can be performed with help of different measurements of real phantoms, or with simulations of the complete scenario and by studying its behavior. The first approach requires a good measurement protocol and less know-how, but the accuracy of the attainable results is severely limited. The second option is viable only if proper models of the system (detectors, chamber, phantoms) are available, but it also allow for a higher degree of versatility in the possible configurations, since it is not bound by available phantoms or instrumentation. The latter approach was chosen for this work, since no supporting mechanics for the detectors was available and because it was decided to keep the highest degree of flexibility in the definition of the system. As result, an accurate model of the detector had to be produced. The software chosen was MCNPX, a tool for Monte Carlo simulations of different particles.

Being the datasheets not always very accurate (see [3]), the reference drawings were used only for the first iteration of the model, then improved through the use of different measurements: point sources (^{241}Am , ^{137}Cs and ^{60}Co) placed on an array of nodes in front of the crystal to estimate the counting efficiency, and a collimated ^{241}Am source scanning along the lateral and front side of the detector to check the alignment of the crystal within the housing. The position of the crystal was found to agree with the specification within the uncertainties, but the measured detection efficiencies differed, in certain points of the array significantly. One source of the deviations was found to be the incorrect model of the corners

of the aluminum case: the reference drawings represented it as curved surface, but a more realistic model with a double inner structure, able to hold firmly the carbon epoxy window, was expected. By contacting the manufacturer again it was possible to get improved drawings, then used to improve MCNPX model and the results of the simulations.

3 Development of the PBC configuration

Being the system completely new and the mechanics not yet defined, the initial optimization of the partial-body counter was performed for both the sitting and the stretched configurations.

The reference virtual phantom used for the task was MeetMan, based on the Visible Human project and available only in stretched configuration. To adapt it to the sitting setup, the phantom was cut into four blocks. Using this model, multiple simulations were performed, changing the source organ (muscles, liver, lungs, gastro-intestinal tract, bones) and the energy of the emitted photons, according to the spectrum of standard nuclides (i.e. ^{241}Am , ^{137}Cs , ^{60}Co). No detectors were placed around the phantom, only the full-energy photon flux in free air was tracked (see figure 1 for an example). The results were used to plot iso-photon-flux surfaces, in turn used to define the optimal regions of space for the positioning of the detectors. New simulations with the detectors placed in the virtual world were performed and the final counting efficiencies estimated. The choice between the different subject sitting positions was performed by comparing the minimum detectable activities (MDA) according to ISO 11 929. The MDA require the local peak background in addition to the counting efficiency, therefore additional simulations including ^{40}K distributed in all organs were performed and the Compton background estimated. This value was summed to the natural background measured in the empty chamber. These three values were used to estimate the MDA of the new system for different nuclide/organ measurement scenarios. The sitting setup was found to offer comparable or better performances in a smaller space with the need of a simpler supporting mechanics. Therefore, it was chosen as configuration for the new system. For more information on the topic, see [3]. Four measurement setup were defined: skull (useful for bone-seeking nuclides), liver, lungs and gastro-intestinal tract.

Using the constraints imposed by these setups, the supporting mechanic for the detectors was designed, a test portal built and the results produced with the previous simulations validated. Given the routine operation of the IVM laboratory, it was decided to avoid the downtime associated with the complete upgrade of the counting system: a stretcher able to be used also with the current phoswich system was bought. This new stretcher was modeled with MCNPX in the reclined configuration and introduced in the subsequent simulations.

4 Development of a WBC configuration

While the mechanics was being designed and built for the first tests, the WBC configuration was developed.

The optimization of this configuration was not straightforward as the previous step, because in WBC applications there are two different and opposite goals: high counting efficiency but also low dependence of the counting efficiency from the position of the contamination, because the biokinetic changes the distribution of the source depending on the time since the intake. In PBC the only goal is only to improve the direct counting efficiency for the selected organ while reducing all the other contributions.

The definition of the counting setup was performed in different steps. First new simulations were performed, using as source different organs (one per simulation) in different phantoms. Different phantoms representing different body sizes and shapes were used for the task, not only MeetMan: the Godwin and Klara phantoms from HMGU had been recently acquired and they were put to use. Several photon energies were taken into account for each organ/phantom combination and the result was a series of over 70 datasets. Again, the (uncollided) photon flux in space around the phantom was tracked, but this value alone was not useful for the chosen goal. Therefore, the standard deviation among selected groups of simulations and the average photon flux were calculated: they are related, respectively, to the dependence of the counting efficiency from the position of the source and to the counting

efficiency. As example, figure 2 shows the results of the simulations with a ^{40}K source in the different organs of the different phantoms. The photon fluxes were merged and the resulting iso-average flux surfaces plotted. In the same figure the region of space where the standard deviation is lower than a specified threshold is also marked. The iso-efficiency surfaces generated by the single organs are smoothed out and the resulting averages appear as uniform shells around the phantom. The region of space with low standard deviation has a cone-like shape, starting near the “focus point” of the arc-like reclined stretcher and expanding as the distance from the phantom increases. This behavior is expected, because the regions of space close to the phantom are characterized by detection efficiencies strongly dependent on the position and shape of the source, no more critical for higher detector-source distances. Figure 3 is another example, representing only plots the iso-standard-deviation surfaces for a 1460 keV source placed in different organs of different phantoms.

To ease the definition of the placement of the detectors, standard deviation and average flux were again merged using the formula:

$$C = k \cdot \log \text{eff} - \text{stddev}$$

with $k > 0$.

The resulting weight value is plotted and used to graphically show the compromises between high detection efficiency and low standard deviation: the higher the value, the better the compromise, see figure 4.

The final detector configuration was hand tuned manually using these results but also trying to keep the position of the detectors balanced between left and right, in order to reduce the influence of lateral shifts of the subject on the final counting efficiency. One detector (behind the back) is dedicated only to the detection of the lowest contaminations, ignoring the effects of the standard deviation.

The final configuration is plotted in figure 5 and a photo representing the same setup is shown in figure 6. Further information is available in [4].

5 Test measurements

Different tests were performed with the new system to test its capabilities. Three of them are described here.

The first one aimed to estimate the MDA for lung measurements, to compare it with the value of the previous system and to have a reference value for routine monitoring of workers. The efficiency calibration was performed with a physical LLNL torso phantom loaded with ^{241}Am in the lungs without additional chest plates. The estimation of the natural Compton background in the 60 keV region was performed by measuring two different unexposed and uncontaminated subjects with the same detector geometry. The results are promising: two detectors alone, placed in front of the chest, are able to attain MDA values comparable to the ones of previous system (5.8 Bq ^{241}Am with the HPGe, 5-7 Bq with the scintillators for a 2000 s measurement). Given the result, it was decided to devote the remaining two detectors to the measurement of other organs, to better define the amount and the location of the contamination instead of trying to decrease the MDA even more. For example, the new reference measurement configuration will have two detectors for the two lungs, one for the liver (whose impulses may affect the activity estimation of the lungs) and one for either skull or knee, both positions suited for the measurement of bone seeking nuclides.

The second test involved the measurement of two subjects potentially contaminated with ^{210}Pb due to past high levels radon exposure. The test was performed with three detectors placed around the skull because the tissue interposed between source and detector does not depend strongly from the body fat. The calibration data were obtained from MC simulations. The resulting MDA (referred to the whole-skeleton content) was 290 Bq or 374 Bq, depending on the potassium content of the subject, values acceptable considered the very low emission probability of the 46.5 keV gamma line (4.25%). This MDA was however too high to detect ^{210}Pb in the two subjects.

The third important test involved the WBC measurement of different subjects returning to Germany after a period in Japan, during which the Fukushima accident happened. Only one of them was contaminated with the radionuclides usually released during such accidents (^{131}I ,

^{132}I , ^{132}Te , ^{134}Cs , ^{137}Cs), but the committed dose was well below the yearly dose to the population: 100 μSv . In this case the new system proved the usefulness of high resolution detectors, since a measurement with the old scintillators was unable to separate the different peaks found in the spectrum: for example, the ^{137}Cs and ^{132}I peaks (662 keV resp. 667 keV) overlaps in a NaI(Tl) spectrum. Figure 7 compares the spectra of one scintillator and one HPGe detector.

6 Conclusions and future work

The system described has been installed, tested and the improved capabilities put to use in different cases. The system has not yet been introduced in the routine operation of the laboratory due to the need of official documentation and complete calibration data, all of them required for the ISO/IEC 17025:2005 accreditation, but it is already being used for the cases where the scintillators are unable to produce reliable results. The introduction in routine is planned for 2012, when also the software for the handling of the routine operations will be ready for operation. The results of these measurements with the two systems can then be used to validate the new counter.

The system described here can and will be improved in different ways. First of all, the MCNPX models can be made more accurate and validated according to quality assurance regulation, to be allowed to replace the physical calibrations: this would make possible a traceable calibration for nuclides, organs and phantoms not available at IVM. Another possible improvement is the connection of the mechanics to a computer to read the position of the detectors in the room and automatically produce input files for the simulations: this would greatly reduce one of the biggest sources of uncertainties, namely the position of the detectors in relation to the subject.

Bibliography

- [1] Marzocchi, O. et al. Comparison of stretched and sitting configurations for partial-body measurements. Applied Radiation and Isotopes, Volume 69 (Proceedings of the 6th CHERNE Workshop), Issue 8, August 2011, Pages 1156–1158. DOI:10.1016/j.apradiso.2010.11.012
- [2] Canberra Industries Inc. Extended Range Coaxial Ge Detectors (XtRa). Retrieved on the 23th of December 2010. <http://www.canberra.com/products/496.asp>
- [3] Mayer, S, Boschung, M, Meier, K, Ladedermann, J-P, and Bochut, F O. Characterisation of the psi whole body counter by radiographic imaging. Radiat Prot Dosimetry (2011) 144 (1-4): 398-401. DOI:10.1093/rpd/ncq322
- [4] Marzocchi, O. et al. Theoretical Assessment of Whole Body Counting Performances Using Numerical Phantoms of Different Gender and Sizes. Radiat Prot Dosimetry (2011) 144 (1-4): 339-343. DOI:10.1093/rpd/ncq319

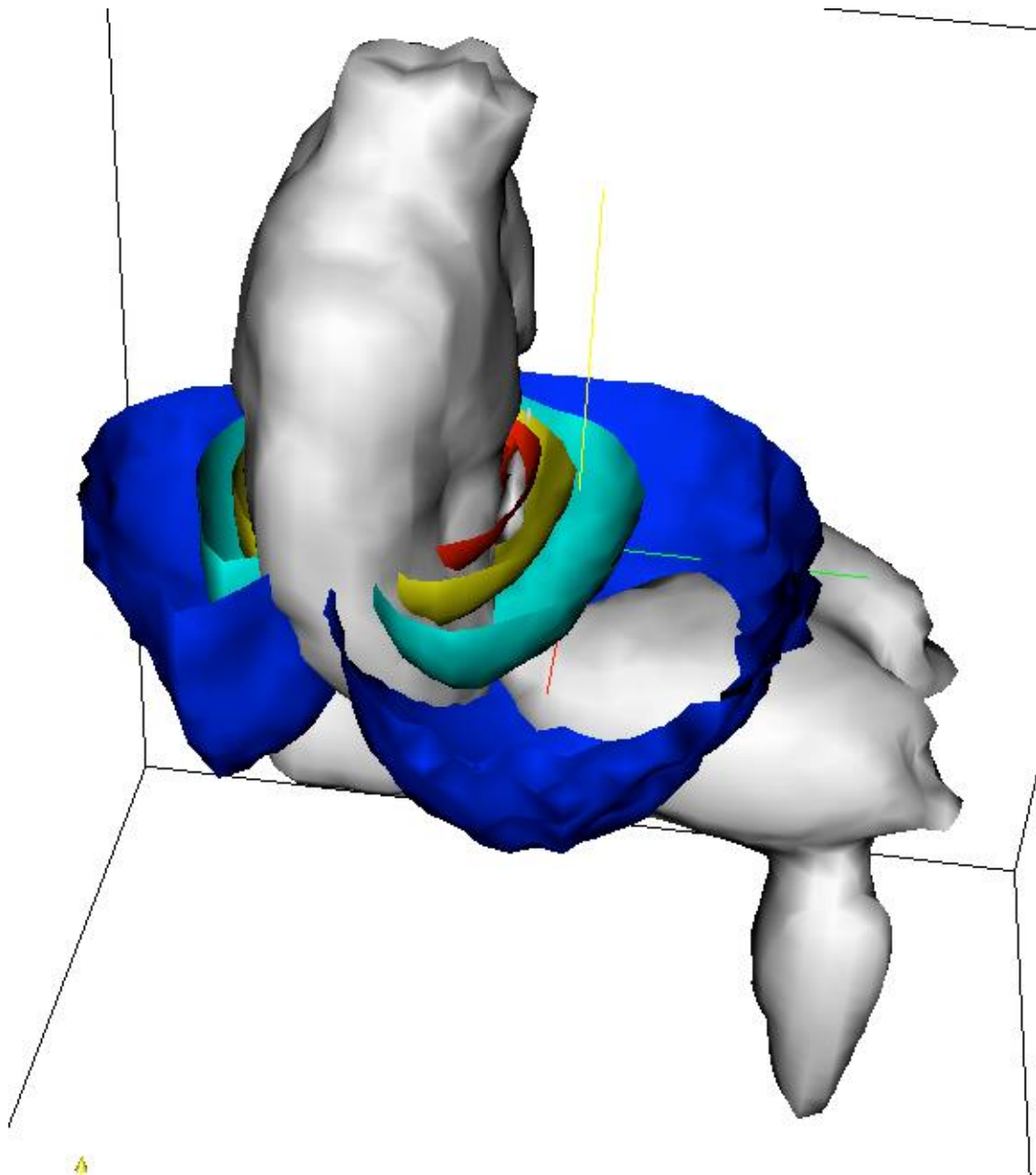


Figure 1 – Plot of the iso-flux surfaces for 60 keV originated by a source in the liver in the MeetMan phantom.

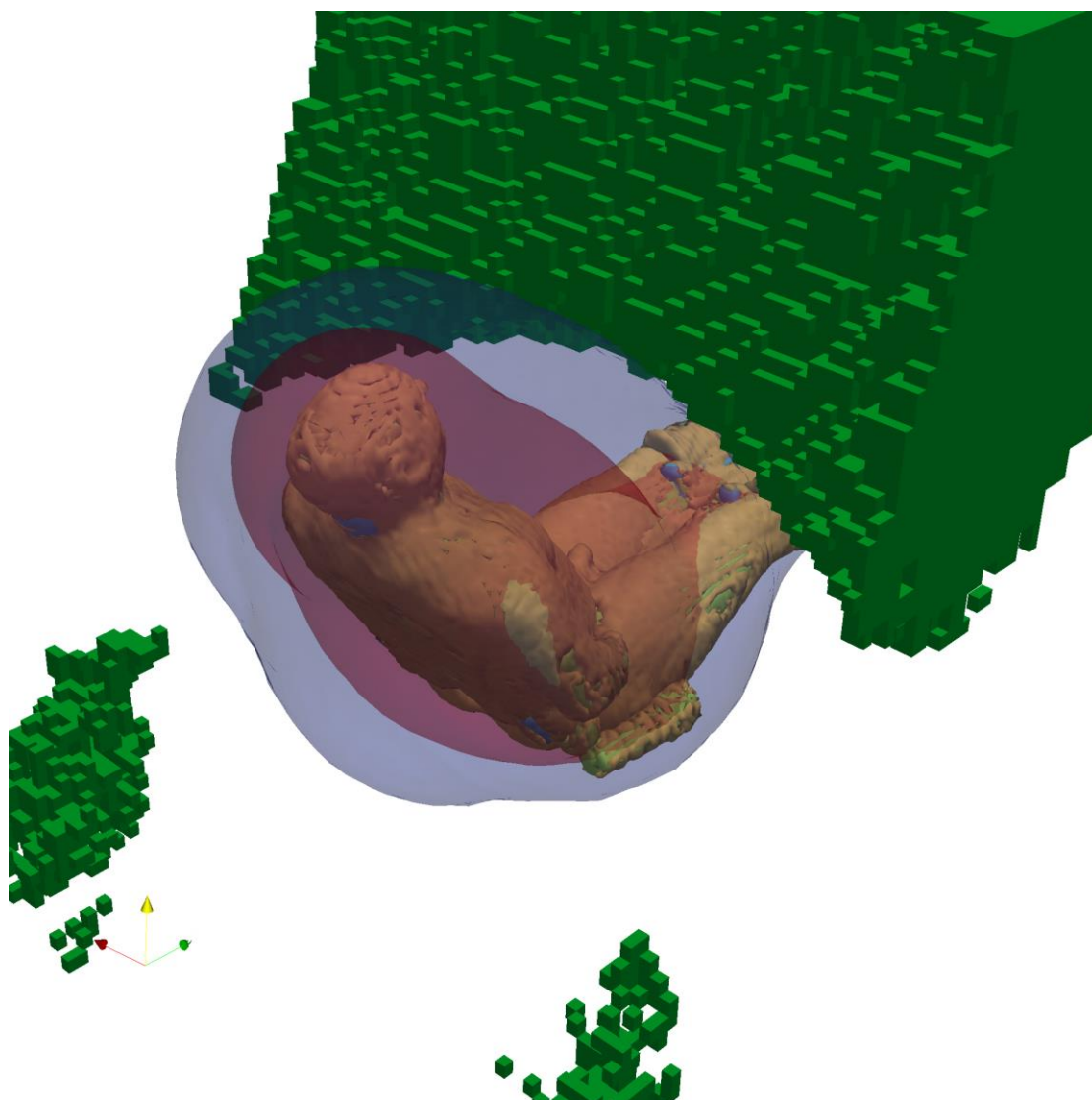


Figure 2 – Plot of the three phantoms used (overlapping each other) and of the iso-flux surfaces resulting from ^{40}K sources distributed in several organs of the phantoms. The green region represents the volume of space where the standard deviation among the detection efficiencies for ^{40}K in the different organs is lower than 20%.

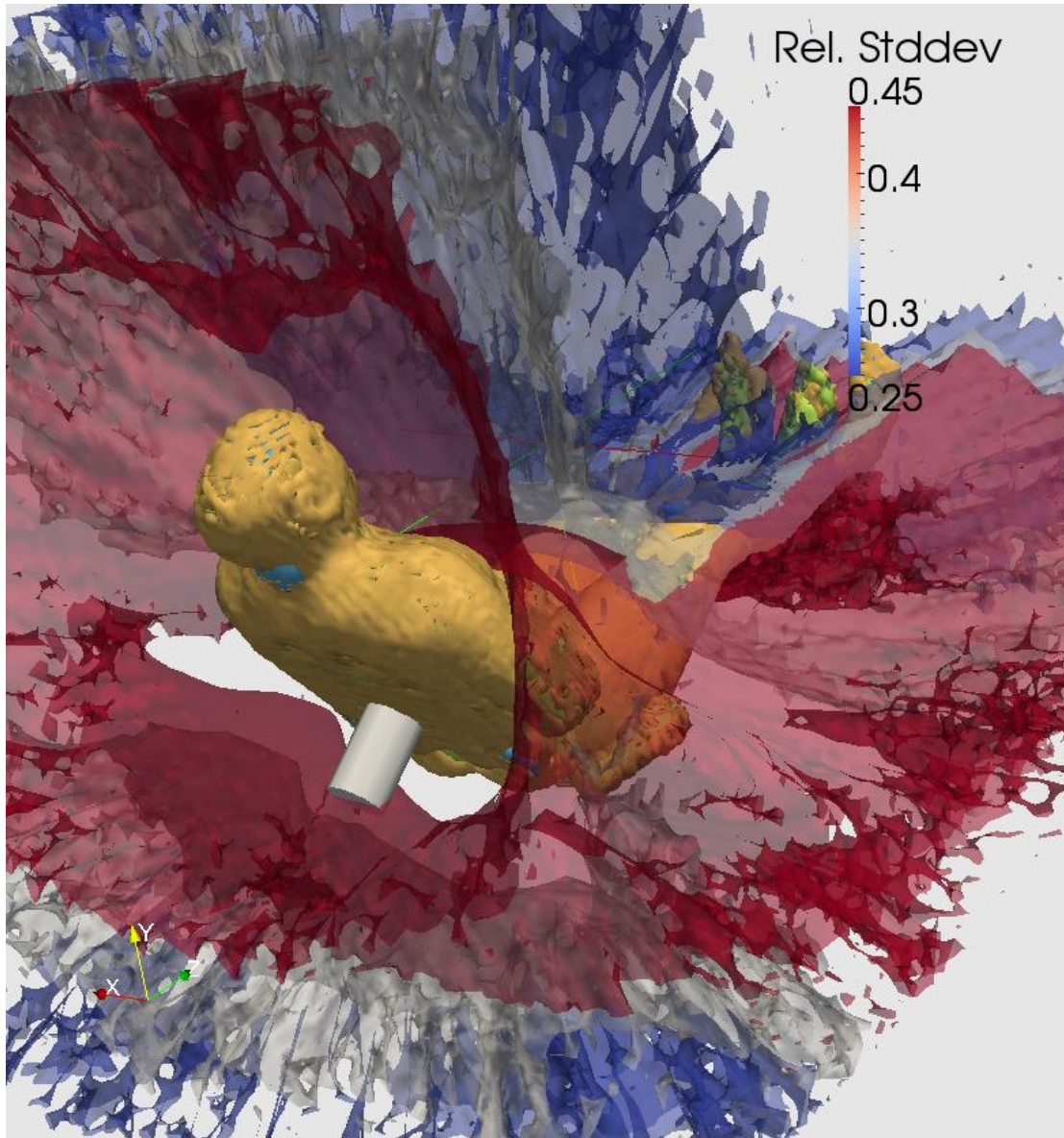


Figure 3 – Plot of the three phantoms used (overlapping each other) and of the standard deviation associated with a dataset that includes all the organs of all the phantoms and an emitter at 1460 keV.

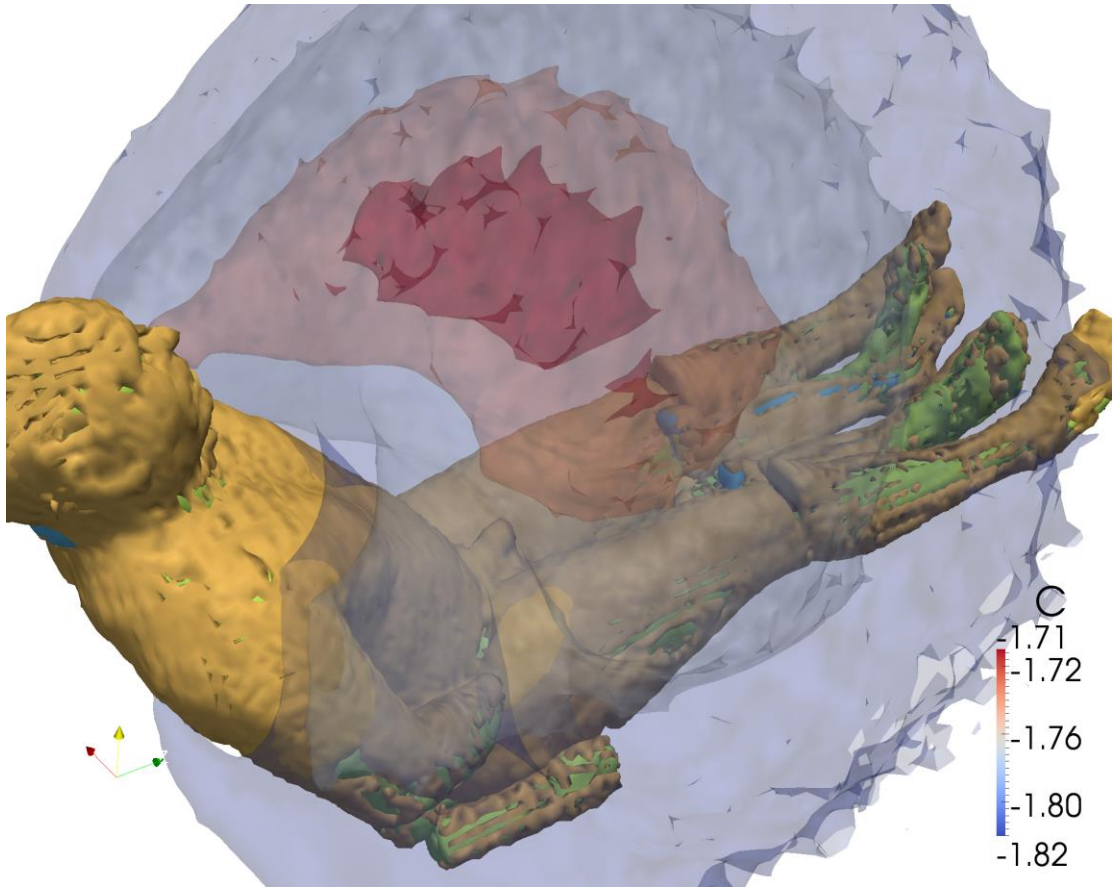


Figure 4 – Plot of the composite value C, resulting from the merge of standard deviation and average efficiencies.

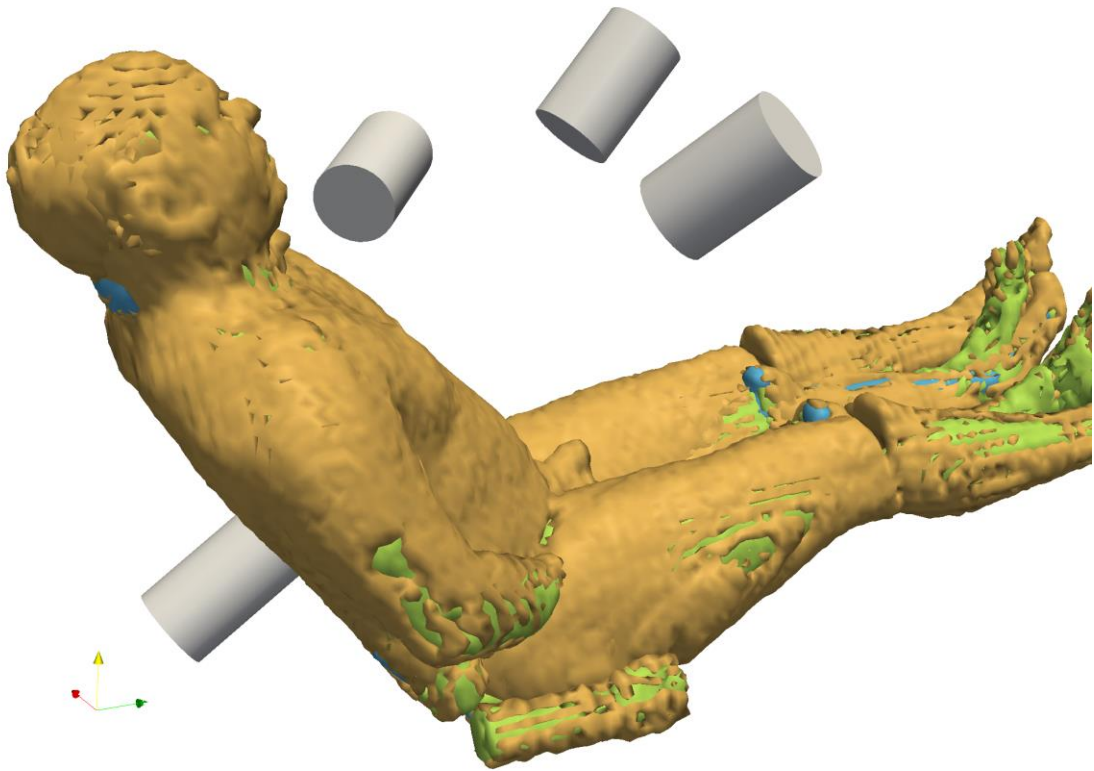


Figure 5 – Position of the detectors in the final WBC configuration.

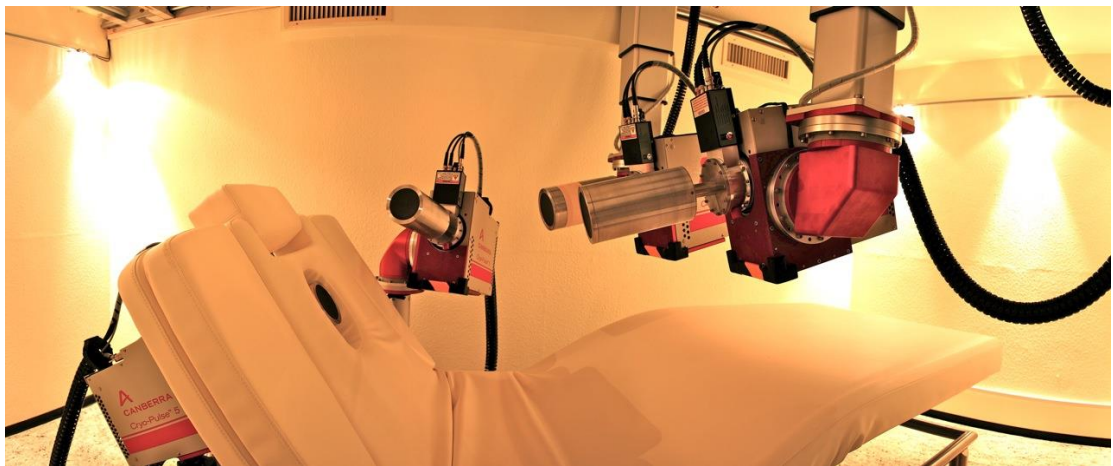


Figure 6 – Panoramic view of the new system in WBC configuration.

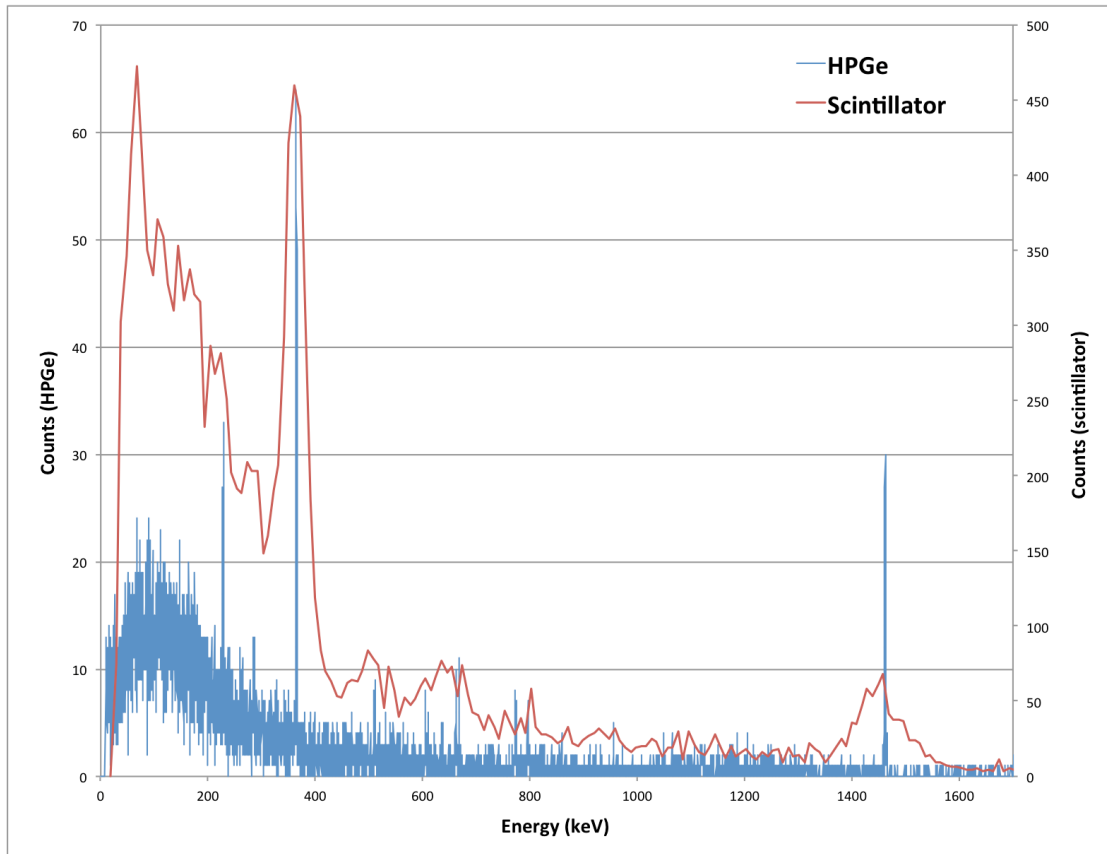


Figure 7 – Comparison of scintillator and HPGe detector spectra (not to scale).